NJC

ROYAL SOCIETY OF CHEMISTRY

PAPER

View Article Online
View Journal | View Issue

Cite this: *New J. Chem.*, 2021, **45**, 4354

Enantiopure methoxetamine stereoisomers: chiral resolution, conformational analysis, UV-circular dichroism spectroscopy and electronic circular dichroism†

Kun Won Lee,‡[a] Ahmed H. E. Hassan, ‡[bc] Youngdo Jeong,[a] Seolmin Yoon,[a] Seung-Hwan Kim,[a] Cheol Jung Lee,[a] Hye Rim Jeon,[a] Suk Woo Chang,[a] Ji-Young Kim,[a] Dae Sik Jang,[a] Hee Jin Kim,[d] Jae Hoon Cheong[e] and Yong Sup Lee *[ac]

Received 23rd October 2020,
Accepted 21st January 2021

DOI: 10.1039/d0nj05192f

rsc.li/njc

The chiral molecule, methoxetamine (MXE), demonstrated promising biological effects in management of treatment-resistant depression patients. To satisfy the need for a method capable of providing gram quantities of each enantiopure stereoisomer of MXE to enable advanced biological studies of enantiomers, a protocol was developed to access gram scale quantities of (*R*)- and (*S*)-MXE in the form of pharmaceutically acceptable HCl salts employing L-(−)-DTTA and D-(+)-DTTA ((−)-*O*,*O*′-di-*p*-toluoyl-L-tartaric acid and (+)-*O*,*O*′-di-*p*-toluoyl-D-tartaric acid, respectively) as two chiral resolving agents. In contrast to ketamine, the measured specific optical rotation and conformational analysis indicated that the most abundant conformers possess a common axial-methoxyphenyl conformation responsible for the conserved direction of optical rotation in both free base and HCl salt forms of the MXE stereoisomers. Finally, the absolute configuration was unambiguously assigned through matching experimental and calculated ECD spectra. This report offers a gateway to obtain gram scale amounts of enantiopure MXE stereoisomers needed to advance the current knowledge on MXE biology.

Introduction

Depression is the most common mental illness that impairs psychosocial functioning and quality of life of hundreds of millions of individuals worldwide. In fact, depression is a complex heterogeneous disease which is provoked by intertwined diverse genetic, epigenetic, developmental and environmental factors.[1,2] The World Health Organization anticipates the burden of major depressive disorder (MDD) will rank first by 2030.[3] Complicated by the partial comprehension of neurobiology of depression and the involvement of multiple molecular targets, the discovery and development of antidepressants has never been a straightforward task. The inception of the monoamine hypothesis in the second half of the 20th century provided a gateway for developing several effective antidepressant agents acting through the monoamine-based mechanism. Monoaminergic-based antidepressants, such as selective serotonin reuptake inhibitors (SSRIs) and serotonin norepinephrine reuptake inhibitors (SNRIs), have been the only available tools to manage depressive disorders for decades.[4] Nevertheless, a significant number of patients are non-responsive to monoaminergic-based antidepressants and, thus, suffer from treatment-resistant depression (TRD, also known as treatment-refractory depression). Evidently, the monoamine hypothesis is not enough to fully explain depression. In addition, the full efficacy of monoaminergic-based antidepressants is achieved only after several weeks. Moreover, several patients show only partial responses. There is a need to consider other mechanism-based targets to develop newer, faster and safer antidepressant agents.

Accumulated evidence has confirmed key roles of glutamate and GABA pathways in depressive disorders, which has opened a gateway to develop a new class of rapid-acting glutamatergic-based

[a] *Department of Life and Nanopharmaceutical Sciences, Kyung Hee University, Seoul 02447, Korea. E-mail: kyslee@khu.ac.kr*
[b] *Department of Medicinal Chemistry, Faculty of Pharmacy, Mansoura University, Mansoura 35516, Egypt*
[c] *Medicinal Chemistry Laboratory, Department of Pharmacy, College of Pharmacy, Kyung Hee University, Seoul 02447, Korea*
[d] *Uimyung Research Institute for Neuroscience, College of Pharmacy, Sahmyook University, Seoul, Republic of Korea*
[e] *School of Pharmacy, Jeonbuk National University, 567 Baekje-daero, Deokjin-gu, Jeonju-si, Jeollabuk-do 54896, Republic of Korea*

† Electronic supplementary information (ESI) available: HRMS and NMR spectra of the compounds. See DOI: 10.1039/d0nj05192f

‡ Both Ahmed H. E. Hassan and Kun Won Lee contributed equally to this work and should be first authors.

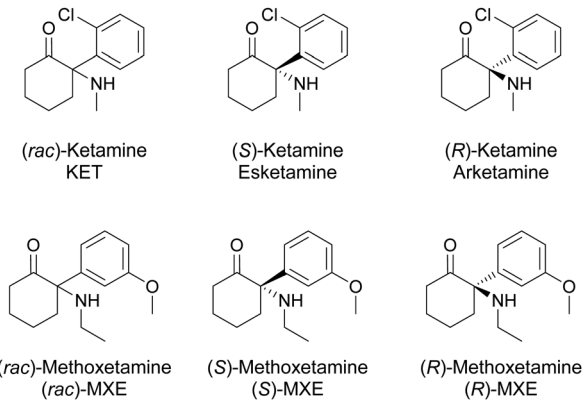

Fig. 1 Chemical structures of racemic and enantiopure forms of ketamine (KET) and methoxetamine (MXE).

antidepressants.[5,6] Basically, three types of ionotropic glutamate receptors have been identified which are NMDA receptors, AMPA receptors and kainate receptors (KARs). The extrasynaptic NMDA receptors inhibit long-term potentiation (LTP) and produce long-term depression (LTD) affecting synaptic plasticity.[7] Accordingly, NMDA receptor antagonists might be promising antidepressant therapeutics which is supported by the reduction of immobility in the forced swim (FST) and tail suspension (TST) tests.[8] Meanwhile, AMPA receptors' activation triggers antidepressant effects and, consequently, AMPA receptor activators might serve as useful antidepressant agents.[9–11]

Recently, ketamine (KET, Fig. 1) was reported as an effective antidepressant for TRD.[12–14] It exhibits rapid and long lasting antidepressant effects mainly through glutamatergic-based-mechanisms, specifically NMDA receptor antagonism and AMPA receptor activation. Studies indicated that KET exerts a rapid-onset and strong effects on TRD and bipolar depression, in addition to minimizing suicidal thoughts. However, KET is a racemic mixture of (*R*)- and (*S*)-enantiomers known as esketamine and arketamine, respectively (Fig. 1). A great concern is that enantiomers possibly elicit different biological responses including therapeutic effects, adverse effects and toxicities.[15,16] Group I of chiral drugs involves chiral drugs whose racemic mixtures are composed of an eutomer, which is the bioactive enantiomer or the enantiomer eliciting the higher pharmacological response, and a distomer which is the less active, inactive or the enantiomer lacking the desired pharmacological response.[17] Meanwhile, group II of chiral drugs involves chiral drugs whose racemic mixtures have equally bioactive enantiomers. Regarding KET enantiomers, esketamine was identified as the eutomer exhibiting 5-fold affinity to the NMDA receptor relative to the distomer arketamine.[18] Accordingly, esketamine has higher efficacy and lower adverse effects and it is capable of alleviating depression in about half of the patients with TRD within two hours demonstrating an action of duration lasting for several days to weeks. In addition, repeated dosing results in a continued relief in responsive patients. In 2019, the FDA approved intranasal esketamine (Spravato®) for the treatment of adults with TRD and then extended its approval in 2020 to include the treatment of adult patients suffering from major depressive disorder (MDD) with acute suicidal ideation or behaviour. Nevertheless, significant drawbacks are associated with KET and esketamine including dissociative symptoms, hypertension and other side effects that last for a few hours post-dose administration. Consequently, esketamine was FDA-approved under a "Risk Evaluation and Mitigation Strategy (REMS)" that necessitates administration of the drug only in licensed clinics or hospitals. In fact, KET is poorly selective as indicated by its affinity to μ-, κ-, and δ-opioid receptors,[19] agonistic activity for σ1 and σ2 receptors,[20] antagonistic activity for muscarinic receptors,[19] and several other biological targets.[21]

Methoxetamine (MXE, Fig. 1) might be a better antidepressant alternative to KET. It possesses a higher NMDA receptor affinity.[22] In addition, it triggers rapid and sustained antidepressant effects similar to KET.[23] Moreover, it shows better selectivity as indicated by the absence of negligible affinities to several off-targets including μ-, κ-, and δ-opioid receptors, σ1 and σ2 receptors. However, MXE is a racemic mixture of (*R*)- and (*S*)-enantiomers. To date, the eutomer and distomer enantiomers of MXE have not been identified. The development of a suitable method for the preparation and enantiomeric resolution of gram-scales of enantiopure MXE stereoisomers is needed to satisfy the demands of biological studies and identify the eutomer and the distomer. This might assist in maximizing the therapeutic effects and minimizing the burden. To meet these needs, we report our efforts towards synthesis, enantioseparation and absolute configuration assignment for the free base forms and the pharmaceutical acceptable HCl salt forms of MXE stereoisomers.

Results and discussion

Synthesis of racemic (*rac*)-MXE HCl salt

(*rac*)-MXE was synthesized *via* modification of the method reported by Jurasek *et al.*[24] As shown in Scheme 1, 3-methoxybenzonitrile (**1**) reacted with the Grignard reagent, cyclopentylmagnesium bromide, similar to the reported method to afford 3-methoxyphenyl cyclopentyl ketone (**2**) in an acceptable yield. Instead of α-bromination employing bromine, as implemented in the reported method, we used copper(II) bromide[25] which afforded α-bromoketone derivative (**3**) in an excellent yield. While the reported method isolated the Schiff base formed *via* the reaction with ethylamine, we advanced the crude α-hydroxyimino-derivative (**4**) to the next step. Importantly, we replaced the poor yielding thermal rearrangement step used in the reported method by palladium(II) chloride-catalysed thermal rearrangement[26] which significantly increased the isolated yield of (*rac*)-MXE after recrystallisation as HCl salt ((*rac*)-MXE HCl) from methanolic hydrochloric acid solution. While the combined yield of Schiff base formation and thermal rearrangement steps used in the reported method was around 16.7%, the yield over the modified two steps of Schiff base formation and palladium(II) chloride-catalysed rearrangement was 49%. ^{1}H NMR, ^{13}C NMR and HRMS data were in agreement with the chemical structure. The overall isolated yield of

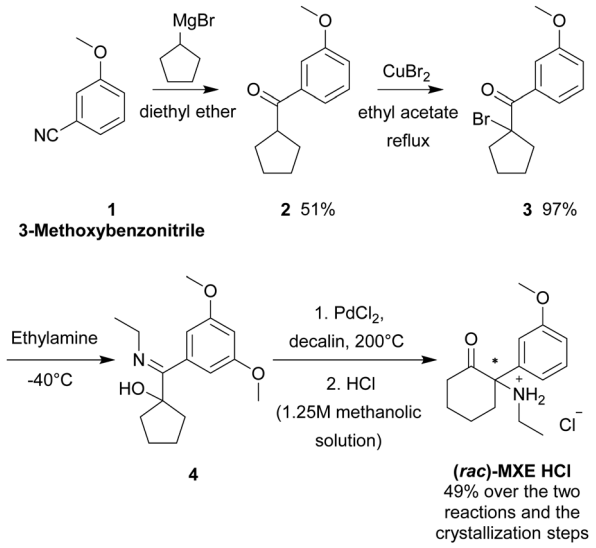

Scheme 1 Synthesis of (*rac*)-MXE HCl.

(*rac*)-MXE HCl after the introduced modifications was 24.2% which is a clearly much improved yield in comparison to the 4.4% overall yield of (*rac*)-MXE of the reported method.[24]

Enantioseparation of (*S*)-MXE and (*S*)-MXE

Chiral resolution of (*R*)- and (*S*)-MXE stereoisomers. Towards the development of a cost-effective and practical chiral resolution protocol capable of yielding gram quantities of the enantiopure MXE stereoisomers, fractional crystallization of the diastereomeric salts was attempted. The reported protocol for enantioseparation of KET stereoisomers using L-(−)-DTTA, (−)-*O*,*O*′-di-*p*-toluoyl-L-tartaric acid,[27] resulted in a poor resolution of MXE stereoisomers, possibly because of the solubility difference between the diastereomeric salts, which was not sufficient to afford crystals of acceptable enantiopurity; in addition to an appreciable solubility of salts in isopropanol used as the solvent for crystallization. Consequently, the use of L-(−)-DTTA as a single resolving agent for MXE stereoisomers resulted in poor enantiopurity and yield (69% ee and 61% yield for (−)-MXE; 32% ee and 32% yield for (+)-MXE). Instead of employing only L-(−)-DTTA as a single resolving agent, a new protocol (Schemes 2 and 3) was developed utilizing two resolving agents; L-(−)-DTTA and D-(+)-DTTA; (+)-*O*,*O*′-di-*p*-toluoyl-D-tartaric acid, for fractional crystallization of the diastereomeric salts from methanolic solutions of salts formed with each chiral resolving agent. For each resolved stereoisomer, the developed protocol involved two sequential fractional crystallization steps to enrich its enantiopurity. Thus, as shown in Scheme 2, (*rac*)-MXE was first converted into L-(−)-DTTA salt in methanolic solution which enabled crystallization of (−)-MXE as a salt of L-(−)-DTTA. To enrich the enantiopurity, a second crystallization step afforded (−)-MXE L-(−)-DTTA salt in 51% yield over the two crystallization steps. To convert to the pharmaceutical acceptable HCl salt, the free (−)-MXE base was liberated *via* treatment with aqueous sodium bicarbonate followed by extraction with toluene and then crystallization from methanolic HCl solution to afford

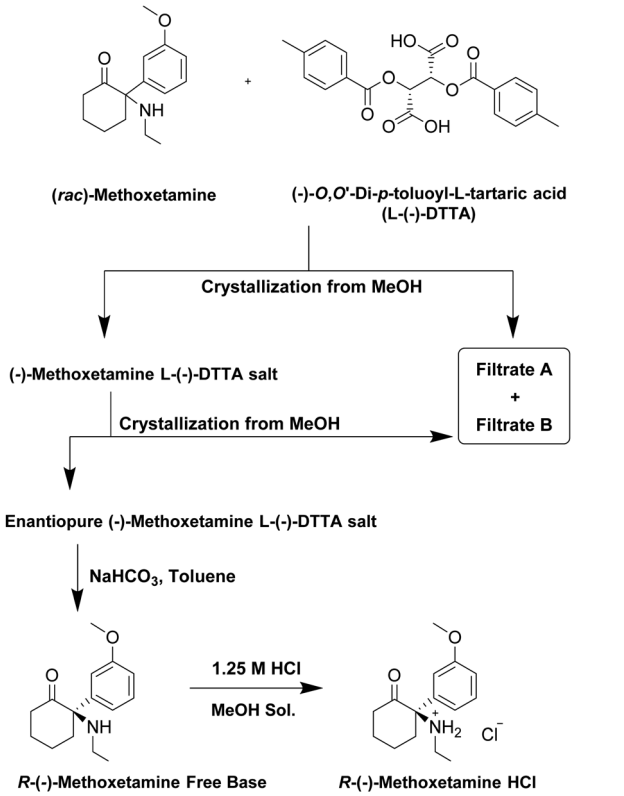

Scheme 2 Established gram scale (*R*)-MXE HCl enantioseparation protocol.

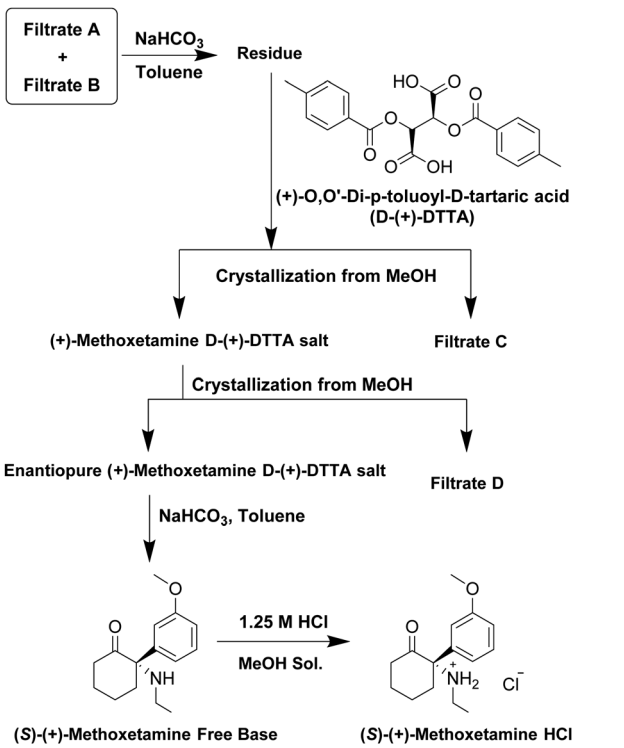

Scheme 3 Established gram scale (*S*)-MXE HCl enantioseparation protocol.

the desired (*R*)-MXE HCl crystals in 91% yield (based on (*R*)-MXE L-(−)-DTTA salt).

To obtain the other stereoisomer as an enantiopure HCl salt, *i.e.* (*S*)-MXE HCl, the recovered filtrates from the two crystallization steps of (*R*)-MXE L-(−)-DTTA (Scheme 3) were combined and treated with sodium bicarbonate to liberate the free base form of MXE. Using the second chiral resolving agent, it was converted into D-(+)-DTTA salt which yielded (*S*)-MXE D-(+)-DTTA crystals upon crystallization from methanol. Again, a second crystallization step towards enrichment of enantiopurity afforded the desired (*S*)-MXE D-(+)-DTTA crystals in 57% yield over two crystallization steps. Herein also, the liberation of the free base form using aqueous sodium bicarbonate and extraction by toluene followed by crystallization from methanolic HCl solution afforded the pharmaceutical acceptable form (*S*)-MXE HCl crystals in 91% yield (based on (*S*)-MXE D-(+)-DTTA salt).

Employing our established chiral HPLC conditions shown below, the excellent enantiopurities of the obtained crystals were confirmed (98% ee and 99% ee for the first and the second isolated stereoisomers, respectively; Fig. S6, ESI†). The measurement of optical properties demonstrated that the first isolated stereoisomer demonstrated levorotatory properties in all of the assessed free base and salt forms (specific optical rotation values of −11.1°, −4.8°, −15.1° and −170° for the free base form in DMF solution, L-(−)-DTTA salt form in DMF, and HCl salt form in ethanolic and aqueous solutions, respectively; Table 1). Meanwhile, the second isolated stereoisomer was confirmed to exhibit dextrorotatory properties in all of the assessed free base and salt forms (specific optical rotation values of +11.8°, +6.2°, +14.7° and +165° for free base form in DMF solution, L-(−)-DTTA salt form in DMF, and HCl salt form in ethanolic and aqueous solutions, respectively; Table 1). This maintenance of the optical rotation direction is a notable behaviour distinguished from the previously reported inversion of optical rotation direction that has been observed for KET free base and HCl forms. The molecular basis for the observed optical rotation inversion in the case of KET stemmed from the fact that the equatorial-chlorophenyl conformation is the most-stable conformer of the free base form while the axial-chlorophenyl conformation is the most-stable conformer of the HCl salt form.[28,29] It might be inferred from the obtained results herein that a similar most stable conformer might be shared between the free base and the corresponding salt forms investigated of MXE. In addition, the large difference in specific rotation between aqueous and ethanolic solutions of the salt form might be a reflection of the impact of solvent effects on specific rotation.[30] As will be shown below, the assignment of absolute configuration proved that the first isolated stereoisomer is (*R*)-(−)-MXE HCl while the second isolated stereoisomer is (*S*)-(+)-MXE HCl.

Establishment of chiral chromatographic conditions for enantioseparation of free and salt forms of (*R*)- and (*S*)-MXE. The development of a chromatographic method for chiral resolution of the various forms of free base and salts of (*R*)- and (*S*)-MXE enantiomers can serve both preparative and analytical purposes. At an analytical scale, it can be a suitable tool to assess the enantiopurity of the resolved enantiomers. In addition, it can be extrapolated to large-scale preparative enantioseparation towards obtaining an enantiopure drug. However, such chromatographic conditions have not been established yet for MXE. A chiral HPLC condition was reported for KET using a CHIRALPAK® IA column, which is an amylose-based chiral stationary phase bearing spatially organized 3,5-dimethylphenylcarbamates on the stereochemically oriented hydroxyl groups, and *n*-hexane/dichloromethane/diethylamine (75/25/0.1) as a mobile phase.[31] Having the more polar methoxy substituent at the 3-position instead of non-polar chloro substituent at the 2-position of KET, the molecular structure of MXE is distinct from KET. Consequently, significant affinity changes of MXE enantiomers towards stationary and mobile phases might arise. In addition, the positively charged nitrogen atom in the case of MXE salts might be another factor that can induce affinity differences relative to KET as the reported method was developed for KET's uncharged free base form. Moreover, the dichloromethane-based mobile phase used in the reported method employed for KET bears several inherent disadvantages including its limited UV transmission levels (transmittance of only 5% at 230 nm) rendering it incompatible with diode-array detectors.[32] Therefore, we started to develop new chiral HPLC conditions for enantioseparation of the free base and salt forms of (*R*)- and (*S*)-MXE enantiomers. First, we started to establish chiral chromatographic conditions for enantioseparation of the free base form of MXE. Eight amylose/cellulose-based chiral stationary phases bearing structurally different carbamates spatially organized on the stereochemically oriented hydroxyl groups (CHIRALPAK® IA-3, IB-3, IC-3, ID-3, IE-3, IF-3, IG-3 and IH-3) were screened using two different mobile phase systems (acetonitrile/Dist. water (60/40) and ethanol/diethylamine (100/0.1)). Configurationally, amylose is poly(α-D-glucopyranoside) while cellulose has the inverted

Table 1 Overall yields, enantiomeric excess and specific optical rotation values of the resolved MXE HCl stereoisomers

	(−)-MXE L-(−)-DTTA	(+)-MXE D-(+)-DTTA	(−)-MXE Free base	(+)-MXE Free base	(−)-MXE HCl	(+)-MXE HCl
Yield[a]	1.57 g, 51%	1.76 g, 57%	—	—	0.64 g, 46%	0.72 g, 52%
ee[b]	—	—	—	—	98%	99%
$[\alpha]_D^{25}$ (*c* 1.0, DMF)	−4.8°	+6.2°	—	—	—	—
$[\alpha]_D^{25}$ (*c* 1.0, EtOH)	—	—	−11.1°	+11.8°	−15.1°	+14.7°
$[\alpha]_D^{25}$ (*c* 0.1, H_2O)	—	—	—	—	−170°	+165°

[a] Yield was calculated based on the free base form of (*rac*)-MXE employed for enantioseparation assuming 100% of each enantiomer. [b] ee: enantiomeric excess.

anomeric stereochemical configuration; *i.e.* poly(β-D-glucopyranoside). The employed stationary phases CHIRALPAK® IB-3 and IC-3 were based on cellulose bearing 3,5-dimethylphenylcarbamate or 3,5-dichlorophenylcarbamate, respectively, spatially organized on the stereochemically oriented hydroxyl groups (Fig. S1, ESI†). Meanwhile, stationary phases CHIRALPAK® IA-3, ID-3, IE-3, IF-3, IG-3 and IH-3 were based on amylose bearing 3,5-dimethylphenylcarbamate, 3-chlorophenylcarbamate, 3,5-dichlorophenylcarbamate, 3-chloro-4-methylphenylcarbamate, 3-chloro-5-methylphenylcarbamate or (*S*)-α-methylbenzylcarbamate, respectively, spatially organized on the stereochemically oriented hydroxyl groups (Fig. S1, ESI†). The variation in the stereochemical configuration of the stationary phase combined with the diversely substituted carbamates spatially organized on the stereochemically oriented hydroxyl groups of these stationary phases is anticipated to demonstrate different affinities towards enantiomers enabling differentiation of MXE (*R*)- and (*S*)-enantiomers. We observed that CHIRALPAK® IA-3, the column reported to resolve the free base form of (*R*)- and (*S*)-KET enantiomers, failed to resolve the free base form of (*R*)- and (*S*)-MXE enantiomers upon using both of the employed mobile phase systems. Switching to CHIRALPAK® IB-3, a cellulose-based stationary phase, *i.e.* the inverted anomeric stereochemical configuration, while maintaining the same carbamate residue of CHIRALPAK® IA-3, failed also to resolve free base forms of (*R*)- and (*S*)-MXE enantiomers. The use of any of the two employed mobile phase systems while replacing the 3,5-dimethylphenylcarbamates of CHIRALPAK® IA-3 and IB-3 by 3,5-dichlorophenylcarbamate failed also to resolve the free base form of (*R*)- and (*S*)-MXE enantiomers regardless of being spatially organized on the stereochemically oriented hydroxyl groups of α- or β-anomeric configurations, *i.e.* CHIRALPAK® IC-3 or IE-3. Accordingly, we focused on the stationary phases based on α-anomeric configuration; *i.e.* amylose, bearing diverse carbamate residues, 3-chlorophenyl, 3-chloro-4-methylphenyl, 3-chloro-5-methyl or (*S*)-α-methylbenzyl derivatives of carbamate moiety (CHIRALPAK® ID-3, IF-3, IG-3 or IH-3). None of them could resolve (*R*)- and (*S*)-MXE enantiomers when the employed mobile phase was acetonitrile/dist. water (60/40). Only 3-chloro-5-methylphenylcarbamate spatially organized on the stereochemically oriented hydroxyl groups of amylose, *i.e.* CHIRALPAK® IG-3 could resolve successfully the free base forms of (*R*)- and (*S*)-MXE enantiomers upon using ethanol/diethylamine (100/0.1) as a mobile phase (Fig. S2, ESI†). Meanwhile the other employed stationary phases having other carbamates spatially organized on the stereochemically oriented hydroxyl groups failed to resolve the free base form of (*R*)- and (*S*)-MXE enantiomers upon using ethanol/diethylamine (100/0.1) as a mobile phase.

Pharmaceutically, salt forms are, in general, more preferable than the free base forms. This might be attributed, at least in part, to their higher stability and better aqueous solubility. In fact, MXE HCl salt might be the practically used pharmaceutical form. Therefore, we addressed the establishment of chiral chromatographic conditions for resolution of its enantiomers. Based on our gained knowledge regarding chromatographic enantioseparation of free base forms of (*rac*)-MXE, we tested the resolution of the (*rac*)-MXE HCl salt form using ethanol/methanol/diethylamine (50/50/0.1) as a mobile phase employing CHIRALPAK® IG-3, the same stationary phase that successfully resolved the free base form. Unfortunately, (*R*)- and (*S*)-enantiomers were not resolved, possibly because of induced alteration of affinity requirements by positively charged nitrogen of the salt form or the change of mobile phase composition. Accordingly, five chiral stationary phases bearing phenylcarbamates having different chloro and/or methyl-substitution patterns spatially organized on the stereochemically oriented hydroxyl groups of amylose/cellulose (CHIRALPAK® IA-3, IB-3, ID-3, IE-3 and IF-3) were evaluated employing ethanol/methanol/diethylamine (50/50/0.1) as a mobile phase. Four stationary phases with either chloro or methyl phenylcarbamate (CHIRALPAK® IA-3, IB-3, ID-3 and IE-3) could not resolve the HCl salt form of MXE enantiomers. Meanwhile, satisfactory enantioseparation was achieved only using the stationary phase bearing spatially organized 3-chloro-4-methylphenylcarbamate on the stereochemically oriented hydroxyl groups of amylose; *i.e.* CHIRALPAK® IF-3 (Fig. S3, ESI†). Next, we checked whether the shift from 3-chloro-5-methylphenylcarbamate (CHIRALPAK® IG-3) to 3-chloro-4-methyl (CHIRALPAK® IF-3) was because of the change in the composition of the mobile phase or the presence of a positively charged nitrogen in the salt form. In this regard, enantioseparation of the free base form of (*rac*)-MXE was evaluated using CHIRALPAK® IF-3 as a stationary phase and ethanol/methanol/diethylamine (50/50/0.1) as a mobile phase. The free base form of (*rac*)-MXE was successfully resolved under these conditions (Fig. S4, ESI†) indicating that the shift from the 3-chloro-5-methyl substitution pattern of the phenylcarbamate (CHIRALPAK® IG-3) to the 3-chloro-4-methyl substitution pattern of the phenylcarbamate (CHIRALPAK® IF-3) might be attributed mainly to the change in the composition of the mobile phase. It also suggests the latter condition as a suitable condition for enantioseparation of both the free base and HCl salt forms of MXE. The universality of these optimized conditions to other salt forms of MXE was checked using enantiopure MXE salts formed with both the L-(−)-DTTA and D-(+)-DTTA. As indicated in Fig. S5 (ESI†), significantly different retention times were observed for each of them. Collectively, these results suggest that the established optimized conditions employing chiral stationary phase CHIRALPAK® IF-3, which is composed of spatially organized 3-chloro-4-methylphenylcarbamate on the stereochemically oriented hydroxyl groups of amylose, in combination with ethanol/methanol/diethylamine (50/50/0.1) as the mobile phase, might serve as universal conditions for chiral chromatographic separation of different forms of MXE.

Conformational analysis of free base and HCl forms of MXE stereoisomers. According to literature reports, two different conformations for KET and KET HCl are responsible for the observed inversion of optical rotation direction. A free KET base form exists in the equatorial-chlorophenyl conformation while KET HCl exists in the axial-chlorophenyl conformation (Fig. 2A).[28,29] In contrast, the found retainability of the direction of optical rotation of MXE enantiomers in both of the free base and its corresponding HCl salt form suggests the

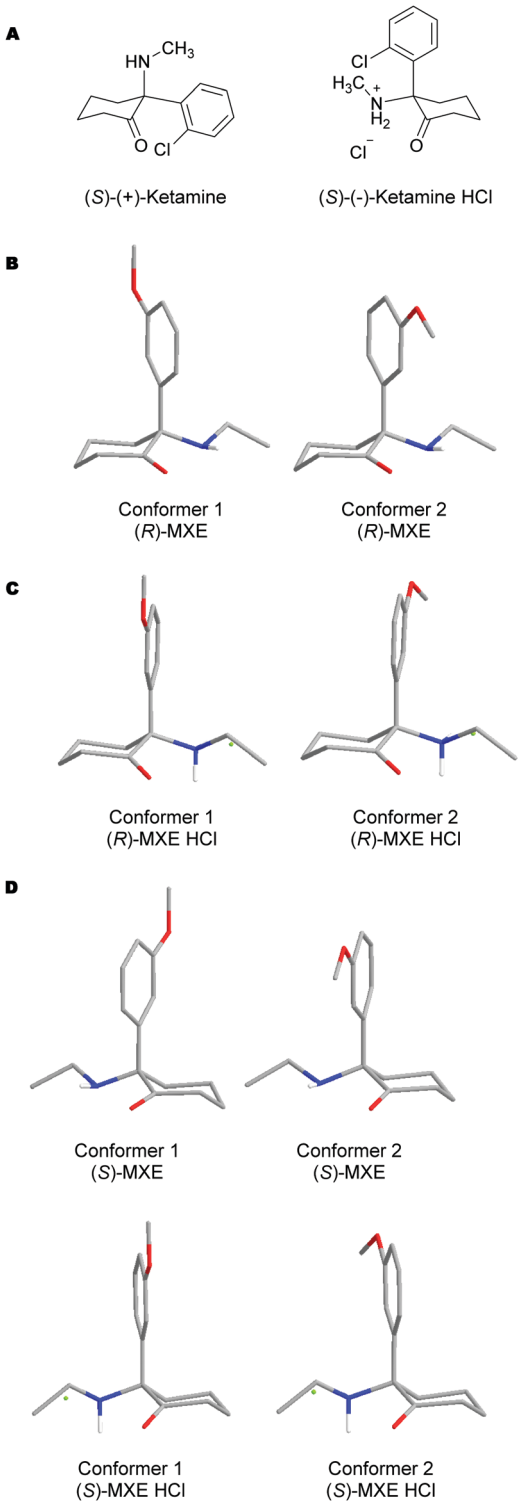

Fig. 2 Most stable conformers of stereoisomers of KET and MXE: (a) reported conformations of free base and HCl salt of (*S*)-KET; (b) calculated most stable conformers of (*R*)-MXE free base form; (c) calculated most stable conformers of (*R*)-MXE HCl form; (d) calculated most stable conformers of (*S*)-MXE free base form; (e) calculated most stable conformers of (*S*)-MXE HCl form.

existence of a common most stable conformer. To check this suggested explanation as a reasonable basis for this phenomenon, conformational analysis of free base and HCl salt forms of (*R*)- and (*S*)-MXE was conducted. In this regard *in silico* calculations employing the systematic conformational search algorithm were conducted using the Merk molecular force field (MMFF). The results showed that an ensemble of 11 conformers represents almost 95% of the conformer populations of the free base form of (*R*)- and (*S*)-MXE while 95% of the conformer populations are represented by only 4 conformers in the case of the HCl salt form of (*R*)- and (*S*)-MXE. As shown in Table 2, only 2 conformers among the 4 most abundant conformers of the free base form of (*R*)- and (*S*)-MXE represented more than 50% of the total conformers' population (populated according to a Boltzmann distribution). As shown in Fig. 2B and C, both of these two conformers for both of (*R*)- and (*S*)-MXE adopt an axial-methoxyphenyl conformation. In case of HCl forms of (*R*)- and (*S*)-MXE, only two conformers represented more than 92% of the total population of conformers (Table 2) and, notably, they were significantly energetically more stable than other conformers. Similar to the most two abundant conformers of the free base form, the conformation of these two conformers showed an axial-methoxyphenyl configuration (Fig. 2D and E). These results are consistent with the inferred existence of a shared common conformation between the free base and the HCl salt form responsible for the retainability of the direction of optical rotation which contrasts the inversion of the direction of optical rotation in

Table 2 Relative energies of the four most abundant conformers among the generated conformers populated according to the Boltzmann distribution

Stereoisomer	Conform.	Relative energy (kJ mol^{-1})	Boltzmann weights	Cumulative Boltzmann weights
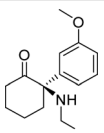 (*R*)-MXE	**1**	**0.00**	**0.278**	**0.278**
	2	**0.35**	**0.241**	**0.518**
	3	2.62	0.096	0.615
	4	2.80	0.090	0.704
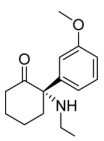 (*S*)-MXE	**1**	**0.00**	**0.278**	**0.278**
	2	**0.35**	**0.241**	**0.519**
	3	2.62	0.097	0.616
	4	2.80	0.090	0.706
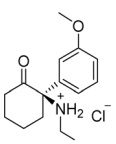 (*R*)-MXE HCl	**1**	**0.00**	**0.516**	**0.516**
	2	**0.58**	**0.409**	**0.925**
	3	8.44	0.017	0.942
	4	8.60	0.016	0.959
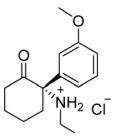 (*S*)-MXE HCl	**1**	**0.00**	**0.516**	**0.516**
	2	**0.58**	**0.409**	**0.925**
	3	8.44	0.017	0.942
	4	8.60	0.016	0.959

the case of free base form of KET's stereoisomers relative to their corresponding HCl salts.

Assignment of absolute configurations of free base and HCl forms of MXE enantiomers. Towards assigning the absolute configuration of the isolated MXE enantiomers as free bases and HCl forms, experimental circular dichroism (CD) spectra of the separated enantiomers were acquired and compared to the calculated electronic circular dichroism (ECD) spectra of (*R*)- and (*S*)-MXE enantiomers as free bases and HCl salts. Because of the high cost of *ab initio* calculations, there is a need to implement calculation methods with acceptable cost-accuracy compromise. Accordingly, we have employed the sufficiently accurate and cost-effective time-dependent density functional theory (TDDFT) method.[33] Selecting a suitable combination of functional/basis set is important for TDDFT calculations. It is noteworthy that benchmarking studies have shown that the performance of range-separated hybrid functions such as CAM-B3LYP is better than the just hybrid functions such as B3LYP for the calculation of ECD spectra.[34] In addition, using Ahlrichs basis sets such as SVP for TDDFT calculations is more reliable than the split-valence Pople basis sets such as 6-31+G. Accordingly, ECD calculations were performed using CAM-B3LYP/SVP as the functional/basis set. Two solvent models were employed in parallel to run separate calculations of ECD spectra. The first solvent model was the "conductor-like polarizable continuum model" (CPCM; calculated ECD spectra are shown in Fig. 3) while the second was the "solvation model based on density" (SMD; calculated ECD spectra are shown in Fig. S7, ESI†).

As shown in Fig. 3, the experimental ECD spectrum of the (−)-MXE free base form displayed a positive cotton effect (CE) at 203 nm ($\Delta\varepsilon$ +10.3) and negative CEs at 227 nm ($\Delta\varepsilon$ −2.8) and 297 nm ($\Delta\varepsilon$ −2.4). This experimental ECD spectrum (Fig. 3) was in agreement with the pattern of the calculated ECD spectrum using the CPCM solvent model for the *R* model of MXE free base, suggesting the absolute configuration of the (−)-MXE base form as *R*. Meanwhile, the experimental ECD spectrum of the (+)-MXE free base form displayed a negative CE at 205 nm ($\Delta\varepsilon$ −11.3) and positive CEs at 227 nm ($\Delta\varepsilon$ +1.8) and 300 nm ($\Delta\varepsilon$ +1.7). This experimental ECD spectrum (Fig. 3) was in agreement with the pattern of the calculated ECD spectrum using the CPCM solvent model for the *S* model, suggesting the absolute configuration of the (+)-MXE base as *S*. Regarding the (−)-MXE HCl form, there was a positive CE at 205 nm ($\Delta\varepsilon$ +11.9) and a negative CE at 294 nm ($\Delta\varepsilon$ −2.9). In comparison to the CPCM model, ECD spectra calculated using the SMD solvent model for both *R* and *S* models of the MXE free base showed more amplified CEs near the 227 nm and 300 nm wave lengths suggesting that calculations using the SMD model were less accurate relative to the CPCM model (Fig. S7, ESI†).

In case of HCl salts of MXE enantiomers, the experimental ECD spectrum (Fig. 3) was consistent with the calculated ECD spectrum using the CPCM solvent model for the *R* model, suggesting the absolute configuration of (−)-MXE HCl as *R*. In addition, the (+)-MXE HCl form showed a negative CE at 205 nm ($\Delta\varepsilon$ −10.6) and a positive CE at 294 nm ($\Delta\varepsilon$ +2.3), which was consistent with the pattern of the calculated ECD spectrum using the CPCM solvent model for the *S* model, suggesting the absolute configuration of (−)-MXE HCl as *S*. In comparison to the CPCM model, the ECD spectra calculated using the SMD solvent model for both *R* and *S* models of MXE HCl salts did not show the pronounced CE observed at 205 nm in the experimental CD spectra (Fig. S7, ESI†).

In summary, the absolute configurations were unambiguously assigned based on matching experimental CD spectra with ECD spectra calculated by employing the CPCM solvent model. Meanwhile, the ECD spectra calculated using the SMD solvent model were less reliable for assignment of absolute configuration of MXE enantiomers. In addition, the calculations employing the SMD solvent model for MXE HCl salts were of much lower accuracy relative to calculations of MXE free bases. Collectively, these results confirm that there is no inversion of the direction of optical rotation between the free base and HCl salt forms of MXE which is distinct from the case of KET.

Experimental

Chemistry

General. All commercially available reagents and solvents were purchased and used without further purification. All reactions were monitored by thin-layer chromatography using E. Merck silica gel 60 F_{254} precoated plates (0.25 mm; Darmstadt, Germany). The TLC spots were visualized under a UV lamp or using staining solutions such as *p*-anisaldehyde solution and ninhydrin solution. ^{1}H and ^{13}C NMR spectra were recorded on a Bruker Avance 400 spectrometer (400 MHz) or a JEOL JNM-ECZ500R spectrometer (500 MHz). Chemical shifts (δ) are reported in ppm relative to tetramethylsilane (0 ppm). High resolution mass spectra (HRMS) were recorded on a Jeol AccuTOF (JMS-T100TD) equipped with a DART (direct analysis in real time) ion source from ionsense, Tokyo, Japan in the positive modes. Optical rotations were measured by using a Jasco P-2000 polarimeter (light source = Na, 589 nm; Hackettstown, USA). Enantiomeric purity assay was carried out by using an optimized chiral HPLC using Agilent 1100 Series Capillary LC (Waldbronn, Germany) using Chiralpak® (3 μm particle size, 4.6 mm × 150 mm; Tokyo, Japan) as a stationary phase and ethanol/methanol/diethylamine = 50 : 50 : 0.1 as a mobile phase in isocratic gradient runs at 0.4 mL min^{-1}. Electronic circular dichroism (ECD) spectra were recorded on a JASCO J-1100(JASCO, Tokyo, Japan) spectropolarimeter.

Preparation of cyclopentyl-3-methoxyphenylketone (2)[24]. 3-Methoxybenzonitrile (1, 4.59 mL, 37.55 mmol) was placed in a round bottom flask under nitrogen. After cooling to 0 °C, cyclopentylmagnesium bromide (2 M diethyl ether solution, 28.17 mL, 56.33 mmol) was added slowly. The reaction temperature was allowed to increase to ambient temperature and the mixture was stirred for 6 hours. The reaction was quenched with HCl (2 N solution, 5 mL) and stirred at ambient temperature for 15 minutes. pH was rendered alkaline with NaOH (2 N solution) then the mixture was extracted with

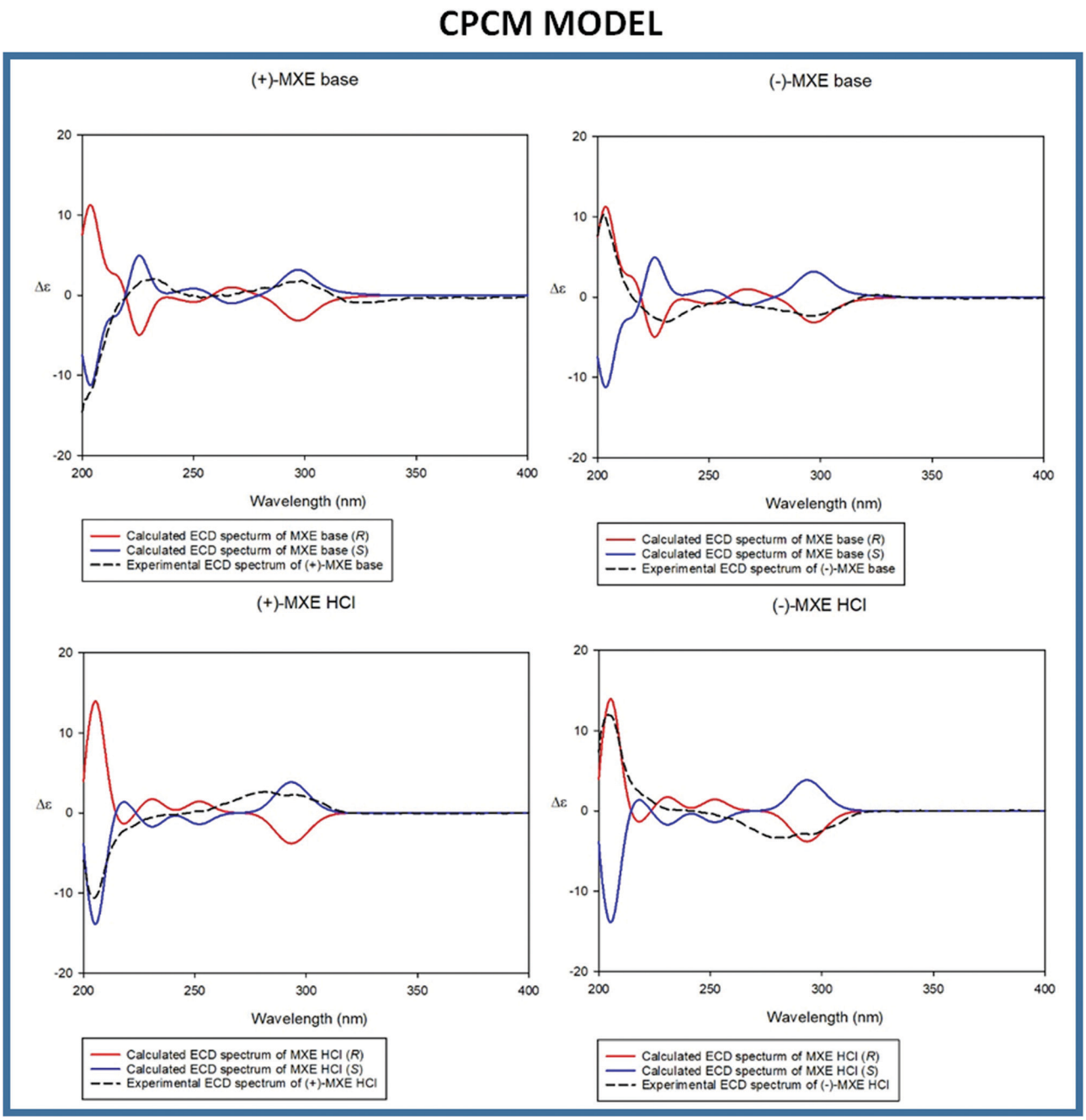

Fig. 3 Comparison of experimental and calculated electronic circular dichroism (ECD) spectra of isolated stereoisomers of MXE free base and their HCl forms using the conductor-like polarizable continuum model (CPCM).

diethyl ether and H_2O. After drying (anhydrous $MgSO_4$) the extract was concentrated under reduced pressure, and purified by column chromatography (EtOAc/*n*-hexane = 1 : 40) to afford compound **2** (3.90 g, 19.09 mmol, 51%).

^{1}H NMR (400 MHz, $CDCl_3$) δ 7.53 (d, J = 7.6 Hz, 1H), 7.49 (t, J = 2.2 Hz, 1H), 7.34 (t, J = 8.0 Hz, 1H), 7.01 (dd, J = 8.2, 2.3 Hz, 1H), 3.82 (s, 3H), 3.67 (p, J = 7.9 Hz, 1H), 1.93–1.84 (m, 4H), 1.73–1.57 (m, 4H).

Preparation of 1-bromocyclopentyl-3-methoxyphenylketone (3)[24]. Compound **2** (3.90 g, 19.09 mmol) was added to a round bottom flask, followed by ethyl acetate (30 mL), and copper(II) bromide (8.53 g, 38.18 mmol). The mixture was heated and stirred under reflux conditions for 4 hours. After cooling to ambient temperature, the reaction mixture was filtered and concentrated. The concentrated filtrate was suspended in hexane, filtered again and then concentrated to obtain compound **3** (5.26 g, 18.58 mmol, 97%) as a crude yellow transparent oil.

^{1}H NMR (400 MHz, $CDCl_3$) δ 7.78 (d, J = 7.6 Hz, 1H), 7.65 (t, J = 2.2 Hz, 1H), 7.35 (t, J = 7.9 Hz, 1H), 7.09 (dd, J = 8.2, 1.9 Hz, 1H), 3.85 (s, 3H), 2.55–2.38 (m, 4H), 2.11–2.00 (m, 2H), 1.85–1.73 (m, 2H).

Preparation of 2-ethylamino-2-(3-methoxyphenyl)cyclohexan-1-one ((*rac*)-MXE) and the corresponding hydrochloride salt ((*rac*)-MXE HCl)[24]. In a sealed tube under a nitrogen atmosphere and cooled to −40 °C an excess of ethylamine was placed. Compound **3** (2.00 g, 7.06 mmol) was added slowly. The reaction mixture was stirred for 6 hours at −40 °C, then the temperature was allowed to increase slowly to ambient temperature and stirred for 12 hours at ambient temperature. The reaction was quenched with water and extracted with diethyl ether. The extract was concentrated under reduced pressure to afford brown oily crude compound **4** (1.75 g) which was dissolved in decalin (8 mL) and placed in a sealed tube. The temperature was increased to 190 °C followed by the addition of palladium(II) chloride (0.1 g) divided into two portions with a two hour interval between additions. After heating for 10 hours, the reaction mixture was cooled, diethyl ether and water were added followed by 4 N HCl to adjust the pH to 2–3. The mixture was extracted three times with diethyl ether followed by the addition of 2 N NaOH to re-adjust the aqueous phase to pH 10–11 then extracted again three times, dried over anhydrous $MgSO_4$, concentrated under reduced pressure and purified by column chromatography (EtOAc/*n*-hexane = 1 : 2) to afford the free base form of methoxetamine (*rac*)-MXE. The free base was converted into the HCl salt through recrystallization from methanolic HCl solution to afford (*rac*)-MXE HCl (0.99 g, 3.50 mmol, 49% over 2 steps) as a white solid.

(*rac*)-MXE: ^{1}H NMR (500 MHz, $CDCl_3$) δ 7.28 (t, J = 7.9 Hz, 1H), 6.82 (d, J = 2.9 Hz, 1H), 6.81–6.79 (m, 1H), 6.77 (t, J = 1.9 Hz, 1H), 3.88 (s, 3H), 2.88–2.84 (m, 1H), 2.41–2.37 (m, 1H), 2.34–2.26 (m, 2H), 2.09–1.92 (m, 4H), 1.87–1.66 (m, 4H), 0.99 (t, J = 7.1 Hz, 3H). ^{13}C NMR (125 MHz, $CDCl_3$) δ 211.27, 160.08, 141.05, 129.89, 119.45, 113.27, 112.35, 69.79, 55.34, 39.82, 36.67, 36.07, 27.68, 22.44, 15.73.

(*rac*)-MXE HCl: ^{1}H NMR (500 MHz, D_2O) δ 7.51 (t, J = 8.3 Hz, 1H), 7.16 (dt, J = 8.6, 2.3 Hz, 1H), 7.01 (d, J = 8.0 Hz, 1H), 6.96 (s, 1H), 3.84 (s, 3H), 3.20 (dd, J = 13.5, 2.6 Hz, 1H), 2.92–2.83 (m, 1H), 2.58–2.45 (m, 3H), 2.06–1.88 (m, 3H), 1.82–1.67 (m, 2H), 1.14 (t, J = 7.2 Hz, 3H); ^{13}C NMR (125 MHz, D_2O) δ 209.01, 160.26, 131.46, 131.07, 120.81, 115.93, 114.13, 72.04, 55.57, 39.01, 37.14, 32.37, 27.38, 21.19, 10.66; HRMS m/z calculated for $C_{15}H_{22}NO_2^+$ $[M + H]^+$ 248.1645, found 248.1671.

Chiral resolution of (*rac*)-MXE into enantiopure stereoisomers

Enantioseparation of (*R*)-(−)-methoxetamine (−)-*O*,*O*′-di-*p*-toluoyl-L-tartarate. (−)-*O*,*O*′-Di-*p*-toluoyl-L-tartaric acid (3.74 g, 9.69 mmol) was added to a methanolic solution (30 mL) of (*rac*)-methoxetamine (2.40 g, 9.69 mmol). The mixture was heated under reflux with stirring for 2 hours, allowed to cool slowly to ambient temperature and set aside to crystallize for 12 hours at room temperature. The crystallized solid (2.16 g, 3.41 mmol) was collected by filtration and the filtrate (filtrate A) was saved for separation of the other stereoisomer. The isolated crystals were recrystallized again from methanol (8 mL) after heating under reflux with stirring then slowly cooled and stood still at ambient temperature for 12 hours. The enantioenriched crystals were collected by filtration to afford (*R*)-(−)-methoxetamine (−)-*O*,*O*′-di-*p*-toluoyl-L-tartarate (1.57 g, 2.48 mmol, 51% yield over two crystallization steps) while the filtrate (filtrate B) was saved for the separation of the other stereoisomer after combination with filtrate A.

White solid; mp: 121–131 °C; $[\alpha]_D^{25}$: −4.8° (*c* 1.0, DMF); ^{1}H NMR (500 MHz, DMSO-d_6) δ 7.84 (d, J = 8.0 Hz, 4H), 7.40 (t, J = 8.0 Hz, 1H), 7.32 (d, J = 8.6 Hz, 4H), 7.02 (dd, J = 8.6, 2.3 Hz, 1H), 6.92–6.89 (m, 2H), 5.65 (s, 2H), 3.76 (s, 3H), 2.98 (d, J = 13.7 Hz, 1H), 2.57–2.52 (m, 1H), 2.36–2.18 (m, 9H), 1.98 (td, J = 13.0, 3.2 Hz, 1H), 1.89–1.87 (m, 1H), 1.73 (d, J = 12.0 Hz, 1H), 1.62–1.49 (m, 2H), 1.04 (t, J = 7.2 Hz, 3H); ^{13}C NMR (125 MHz, DMSO-d_6) δ 207.00, 168.50, 165.41, 160.31, 144.29, 130.97, 129.87, 129.76, 127.39, 120.78, 115.27, 114.42, 72.70, 71.21, 55.74, 37.30, 32.97, 27.30, 21.81, 21.71, 12.25.

Preparation of (*R*)-(−)-methoxetamine hydrochloride acid salt. (*R*)-(−)-Methoxetamine (−)-*O*,*O*′-di-*p*-toluoyl-L-tartarate (1.57 g, 2.48 mmol) was treated with $NaHCO_3$ aqueous solution and extracted three times with toluene, dried (anhydrous $MgSO_4$) and evaporated under reduced pressure. The residue was treated with hydrochloric acid (1.5 eq. of 1.25 M methanolic solution) and stirred at 0 °C for 30 minutes. After evaporation under reduced pressure, it was re-dissolved in methanol (5 mL) and recrystallized from diethyl ether at 0 °C to afford (*R*)-(−)-methoxetamine hydrochloride acid salt (0.64 g, 91% yield, 98% ee, Chiralpak IF-3, EtOH/MeOH/DEA = 50/50/0.1, 0.5 mL min^{-1}, rt: 5.75 min).

White solid; mp: 235–245 °C; $[\alpha]_D^{25}$: −15.1° (*c* 1.0, EtOH, hydrochloride salt); $[\alpha]_D^{25}$: −170° (*c* 0.1, H_2O, hydrochloride salt); $[\alpha]_D^{25}$: −11.1° (*c* 0.5, EtOH, free base); ^{1}H NMR (500 MHz, D_2O) δ 7.51 (t, J = 8.0 Hz, 1H), 7.15 (dd, J = 8.6, 2.3 Hz, 1H), 7.01 (d, J = 8.0 Hz, 1H), 6.95 (s, 1H), 3.84 (s, 3H), 3.20 (d, J = 14.3 Hz, 1H), 2.87 (dt, J = 19.5, 7.4 Hz, 1H), 2.57–2.48 (m, 3H), 2.04–1.92 (m, 3H), 1.80–1.67 (m, 2H), 1.14 (t, J = 7.2 Hz, 3H); ^{13}C NMR (125 MHz, D_2O) δ 209.00, 160.08, 131.36, 131.06, 120.81, 115.93, 114.12, 72.03, 55.57, 39.01, 37.14, 32.37, 27.38, 21.19, 10.66.

Enantioseparation of (*S*)-(+)-methoxetamine (+)-*O*,*O*′-di-*p*-toluoyl-D-tartarate. The residue after evaporation under reduced pressure of the combined filtrates A and B was treated with saturated $NaHCO_3$ (aqueous solution), extracted three times with toluene, dried (anhydrous $MgSO_4$) and re-evaporated under reduced pressure to afford the free base form of methoxetamine as a residue (1.54 g, 6.22 mmol). Methanol (20 mL) and (+)-*O*,*O*′-di-*p*-toluoyl-D-tartaric acid (2.40 g, 6.22 mmol) were added to the obtained free base form. The mixture was heated under reflux with stirring for 2 hours, then allowed to cool slowly to ambient temperature and set aside to crystallize for 12 hours at ambient temperature. The formed crystals (2.19 g, 3.46 mmol) were collected by filtration. The isolated crystals were recrystallized again from methanol (8 mL) after heating under reflux with stirring then slow cooling and standing still at ambient temperature for 12 hours. The formed crystals were collected by filtration to afford (*S*)-(+)-methoxetamine (+)-*O*,*O*′-di-*p*-toluoyl-D-tartarate (1.76 g, 2.77 mmol, 57% yield over two crystallization steps).

White solid; mp: 115.5–125.5 °C; $[\alpha]_D^{25}$: +6.2° (*c* 1.0, DMF); ^{1}H NMR (500 MHz, DMSO-d_6) δ 7.83 (d, J = 8.6 Hz, 4H), 7.40 (t,

J = 8.0 Hz, 1H), 7.31 (d, J = 8.0 Hz, 4H), 7.02 (dd, J = 8.6, 2.3 Hz, 1H), 6.91 (d, J = 8.0 Hz, 1H), 6.88 (d, J = 2.3 Hz, 1H), 5.63 (s, 2H), 3.76 (s, 3H), 2.98 (d, J = 13.7 Hz, 1H), 2.52–2.57 (m, 1H), 2.16–2.39 (m, 9H), 1.88–1.99 (m, 2H), 1.75 (d, J = 11.5 Hz, 1H), 1.50–1.63 (m, 2H), 1.03 (t, J = 7.2 Hz, 3H); ^{13}C NMR (125 MHz, DMSO-d_6) δ 207.51, 168.42, 165.36, 160.26, 144.28, 130.87, 129.84, 127.36, 120.69, 114.95, 114.38, 72.31, 71.10, 55.74, 37.26, 33.62, 27.35, 21.82, 21.70, 12.71.

Preparation of (*S*)-(+)-methoxetamine hydrochloride acid salt. (*S*)-(+)-Methoxetamine (+)-*O*,*O*′-di-*p*-toluoyl-D-tartarate (1.76 g, 2.77 mmol) was treated with $NaHCO_3$ aqueous solution and extracted three times with toluene, dried (anhydrous $MgSO_4$) and evaporated under reduced pressure. The residue was treated with hydrochloric acid (1.5 eq. of 1.25 M methanolic solution) and stirred at 0 °C for 30 minutes. After evaporation under reduced pressure, it was re-dissolved in methanol (4 mL) and recrystallized from diethyl ether at 0 °C to afford (*S*)-(+)-methoxetamine hydrochloride acid salt (0.72 g, 91% yield, 99% ee, Chiralpak IF-3, EtOH/MeOH/DEA = 50/50/0.1, 0.5 mL min^{-1}, rt: 5.30 min).

White solid; mp: 235–245 °C; $[\alpha]_D^{25}$: +14.7° (*c* 1.0, EtOH, hydrochloride salt); $[\alpha]_D^{25}$: +165° (*c* 0.1, H_2O, hydrochloride salt); $[\alpha]_D^{25}$: +11.8° (*c* 0.5, EtOH, free base); ^{1}H NMR (500 MHz, D_2O) δ 7.51 (t, J = 8.0 Hz, 1H), 7.15 (dd, J = 8.6, 1.7 Hz, 1H), 7.01 (d, J = 8.0 Hz, 1H), 6.95 (s, 1H), 3.84 (s, 3H), 3.19 (d, J = 13.7 Hz, 1H), 2.87 (dt, J = 19.5, 7.2 Hz, 1H), 2.57–2.48 (m, 3H), 2.04–1.92 (m, 3H), 1.80–1.67 (m, 2H), 1.14 (t, J = 7.4 Hz, 3H); ^{13}C NMR (125 MHz, D_2O) δ 209.01, 160.08, 131.35, 131.06, 120.80, 115.92, 114.12, 72.03, 55.56, 39.01, 37.13, 32.37, 27.38, 21.18, 10.65.

Conformational analysis and calculation of electronic circular dichroism (ECD) spectra. The 3D models of MXE free base and HCl forms were built using the Chem 3D program. A conformational search was performed using the systematic (ring + spin) stepped method as implemented in Spartan'14 software (Wavefunction, Inc., Irvin, CA, USA; 2014) using the Merk molecular force field (MMFF). The algorithm parameters were set to exclude conformers with energy outside a window of 40 kJ mol^{-1} above the energy of the global minimum conformation. Geometry optimization of the obtained conformers was subsequently performed at the B3LYP/6-31+G(d,p) level by the Gaussian 09 software (Revision E.01; Gaussian, Inc., Wallingford, CT, USA; 2009). Time-dependent density functional theory (TDDFT) electronic circular dichroism (ECD) calculations of the optimized conformers were carried out at the CAM-B3LYP/SVP level with a conductor-like polarizable continuum solvent model (CPCM) where MeCN was the solvent model (Gaussian 09 software).

Conclusions

This work addressed the development of a chiral resolution protocol capable of providing gram scale quantities of both (*R*)- and (*S*)-MXE. First, racemic MXE was synthesized efficiently following a modified scheme affording 5.5-fold the overall yield of the reported synthetic method (24.2% relative to the 4.4% overall yield). Employing two chiral resolving agents L-(−)-DTTA and D-(+)-DTTA and conducting two sequential fractional crystallization steps for each enantiomer afforded in the last steps gram scales of pharmaceutical acceptable HCl forms of both (*R*)- and (*S*)-MXE enantiomers in excellent ee and reasonable yields. In contrast to the reported inversion of optical rotation direction of KET HCl salts relative to the free base form, the results showed retainability of optical rotation direction by the free base and the HCl salt form. This suggested the presence of a common most stable conformer for both of the free base and the HCl salt forms. Conformational analysis confirmed this suggestion indicating that both the free base and salt forms share axial-methoxyphenyl conformation of the most abundant stable conformers. Comparing experimental to calculated ECD spectra unambiguously assigned the absolute configuration of both free base and HCl forms of the resolved MXE enantiomers.

Statement of contributions

Y. S. Lee and J. H. Cheong conceived and designed the study; A. H. E. Hassan, K. W. Lee, Y. Jeong, S. Yoon, C. J. Lee and H. R. Jeon performed the experiments; K. W. Lee and Y. Jeong contributed to acquisition of analytical data; S.-H. Kim, S. W. Chang, J.-Y. Kim and D. S. Jang analyzed data; Y. S. Lee, A. H. E. Hassan and J. H. Cheong drafted and revised the article.

Conflicts of interest

There are no conflicts to declare.

Acknowledgements

We are thankful to Ms Ju-Hyeon Jin from CTK (Chiral Technology Korea) for her help in the chiral HPLC analysis of compounds. This research was supported by the Ministry of Food and Drug Safety (#20201063).

References

1 C. J. Peña and E. J. Nestler, *Prog. Mol. Biol. Transl. Sci.*, 2018, **157**, 41–66.
2 M. Shadrina, E. A. Bondarenko and P. A. Slominsky, *Front. Psychiatry*, 2018, **9**, 334.
3 G. S. Malhi and J. J. Mann, *Lancet*, 2018, **392**, 2299–2312.
4 J. Gordon, New Hope for Treatment-Resistant Depression: Guessing Right on Ketamine, https://www.nimh.nih.gov/about/director/messages/2019/new-hope-for-treatment-resistant-depression-guessing-right-on-ketamine.shtml, (accessed January 2021).
5 B. Kadriu, L. Musazzi, I. D. Henter, M. Graves, M. Popoli and C. A. Zarate Jr, *Int. J. Neuropsychopharmacol.*, 2019, **22**, 119–135.
6 J. H. Krystal, G. Sanacora, H. Blumberg, A. Anand, D. S. Charney, G. Marek, C. N. Epperson, A. Goddard and G. F. Mason, *Mol. Psychiatry*, 2002, 7(Suppl. 1), S71–S80.

7 A. Adell, *Biomolecules*, 2020, **10**, 947.
8 A. Haj-Mirzaian, N. Kordjazy, A. Haj-Mirzaian, S. Ostadhadi, M. Ghasemi, S. Amiri, M. Faizi and A. Dehpour, *Psychopharmacology*, 2015, **232**, 3551–3561.
9 M. K. Seo, L. T. Hien, M. K. Park, A. J. Choi, D.-H. Seog, S.-H. Kim, S. W. Park and J. G. Lee, *Sci. Rep.*, 2020, **10**, 993.
10 C. Yang, W. Zhou, X. Li and J. Yang, *Expert Opin. Invest. Drugs*, 2012, **21**, 583–584; author reply 584–585.
11 D. Bleakman, A. Alt and J. M. Witkin, *CNS Neurol. Disord.: Drug Targets*, 2007, **6**, 117–126.
12 C. F. Zorumski, P. Nagele, S. Mennerick and C. R. Conway, *Front. Psychiatry*, 2015, **6**, 172.
13 L. R. Aleksandrova, A. G. Phillips and Y. T. Wang, *J. Psychiatry Neurosci.*, 2017, **42**, 222–229.
14 N. Llamosas, L. Perez-Caballero, E. Berrocoso, C. Bruzos-Cidon, L. Ugedo and M. Torrecilla, *Prog. Neuropsychopharmacol. Biol. Psychiatry*, 2019, **88**, 243–252.
15 J. McConathy and M. J. Owens, *Prim. Care Companion J. Clin. Psychiatry*, 2003, **5**, 70–73.
16 M. Eichelbaum, *Arch. Toxicol., Suppl.*, 1995, **17**, 514–521.
17 L. A. Nguyen, H. He and C. Pham-Huy, *Int. J. Biomed. Sci.*, 2006, **2**, 85–100.
18 M. W. Tyler, H. B. Yourish, D. F. Ionescu and S. J. Haggarty, *ACS Chem. Neurosci.*, 2017, **8**, 1122–1134.
19 R. Kohrs and M. E. Durieux, *Anesth. Analg.*, 1998, **87**, 1186–1193.
20 M. Narita, K. Yoshizawa, K. Aoki, M. Takagi, M. Miyatake and T. Suzuki, *Addict. Biol.*, 2001, **6**, 373–376.
21 P. Zanos, R. Moaddel, P. J. Morris, L. M. Riggs, J. N. Highland, P. Georgiou, E. F. R. Pereira, E. X. Albuquerque, C. J. Thomas, C. A. Zarate, Jr. and T. D. Gould, *Pharmacol. Rev.*, 2018, **70**, 621–660.
22 B. L. Roth, S. Gibbons, W. Arunotayanun, X.-P. Huang, V. Setola, R. Treble and L. Iversen, *PLoS One*, 2013, **8**, e59334.
23 C. J. Botanas, J. Bryan de la Peña, R. J. Custodio, I. Joy Dela Peña, M. Kim, T. Woo, H. J. Kim, H. I. Kim, M. Chang Cho, Y. S. Lee and J. H. Cheong, *Neuropharmacology*, 2017, **126**, 121–127.
24 B. Jurasek, M. Himl, R. Jurok, K. Hajkova, A. Vobinuskova, P. Rezanka and M. Kuchar, *RSC Adv.*, 2017, **7**, 56691–56696.
25 J. Jose, S. A. Gamage, M. G. Harvey, L. J. Voss, J. W. Sleigh and W. A. Denny, *Bioorg. Med. Chem.*, 2013, **21**, 5098–5106.
26 A. Moghimi, S. Rahmani, R. Zare and M. Sadeghzadeh, *Synth. Commun.*, 2014, **44**, 2021–2028.
27 Y. A. Tawar, R. M. Patil, R. S. Lokhande and D. H. Ner, *Paripex Indian J. Res.*, 2017, **6**, 201–204.
28 B. Chankvetadze, N. Burjanadze, J. Breitkreutz, K. Bergander, D. Bergenthal, O. Kataeva, R. Fröhlich, H. Luftmann and G. Blaschke, *J. Sep. Sci.*, 2002, **25**, 1155–1166.
29 P. Hakey, W. Ouellette, J. Zubieta and T. Korter, *Acta Crystallogr., Sect. E: Struct. Rep. Online*, 2008, **64**, o1487.
30 A. T. Fischer, R. N. Compton and R. M. Pagni, *J. Phys. Chem. A*, 2006, **110**, 7067–7071.
31 C. Yang, Y. Shirayama, J. C. Zhang, Q. Ren, W. Yao, M. Ma, C. Dong and K. Hashimoto, *Transl. Psychiatry*, 2015, **5**, e632.
32 R. Lafont, C. Blais, J. Harmatha and I. D. Wilson, in *Encyclopedia of Separation Science*, ed. I. D. Wilson, Academic Press, Oxford, 2000, pp. 2631–2643, DOI: 10.1016/B0-12-226770-2/06431-0.
33 J. Autschbach, L. Nitsch-Velasquez and M. Rudolph, *Top. Curr. Chem.*, 2011, **298**, 1–98.
34 G. Pescitelli and T. Bruhn, *Chirality*, 2016, **28**, 466–474.

